Late Pleistocene chronology, palaeoecology and stratigraphy at a suite of sites along the Albany River, Hudson Bay Lowlands, Canada

April S Dalton[1*], Sarah A Finkelstein[1], Peter J Barnett[2], Minna Väliranta[3], Steven L Forman[4]

[1] *Department of Earth Sciences, University of Toronto, Toronto, Canada, M5S 3B1*

[2] *Department of Earth Sciences, Laurentian University, Sudbury, Canada, P3E 2C6*

[3] *Department of Environmental Sciences, University of Helsinki, Finland, FIN-00014*

[4] *Department of Geosciences, Baylor University, Waco, Texas, United States, 76798*

*corresponding author at Department of Earth Sciences, University of Toronto, Toronto, Canada, M5S 3B1

Email address: aprils.dalton@mail.utoronto.ca

Abstract

Stratigraphic records from formerly glaciated regions are critical for detailed study of the timing, onset and dynamics of past ice sheets and the palaeoecology of previous ice-free intervals. We examined three stratigraphic sections from an 18-km stretch of the Albany River, Hudson Bay Lowlands, Canada, located at the geographic center for many Late Pleistocene ice sheets. Till characterization and correlation suggest that at least three glacial advances from shifting ice centers within the Labrador sector of the Laurentide Ice Sheet were preserved in these stratigraphic records. Non-glacial units (fluvial, organic-bearing sediments) were constrained via optically stimulated luminescence to two possible periods at ca. 73,000 to 68,000 yr BP and ca. 60,000 yr BP. Boreal and peatland taxa (*Picea, Pinus*, Poaceae, *Betula*, Cyperaceae, *Sphagnum*) dominated the pollen record at each site, whereas plant macrofossils analyzed at one site confirm

the local presence of conifer trees (bark, needles, seed wings), bryophytes (largely *Scorpidium* spp), herbaceous plants (Caryophyllaceae, *Carex*, Poaceae), and an aquatic setting (e.g. *Potamogeton*, ephippia of *Daphnia* spp*)*. Pollen-derived average summer temperature reconstructions suggested that local temperatures at the Albany sites were between 12–15°C, which is similar to present-day estimates for the region (14.2°C). Reconstructed annual precipitation estimates were 580–640 mm, which is similar to slightly higher than present-day estimates (564 mm). Non-glacial intervals at the Albany sites likely represent abandoned fluvial environments that supported water-logged peatland biota. Results from this research contribute toward ongoing efforts to constrain ice sheet dynamics over North America during the last glacial cycle (e.g. 71,000–14,000 yr BP) and provide insight into the complex Late Pleistocene palaeoclimate record at the innermost area of the glaciated region.

Keywords: modern analogue technique, pollen, macrofossils, optically stimulated luminescence, MIS 3, MIS 5, pre-LGM, Wisconsinan Stage

1. Introduction

The Quaternary has been defined by repeated glaciations over the Northern Hemisphere that had large-scale influences on global sea level (Grant et al., 2014), atmospheric processes (Sionneau et al., 2013; Ullman et al., 2014), biotic migration and carbon cycling (Kleinen et al., 2015; Brovkin et al., 2016). These glaciations resulted in a highly fragmented stratigraphic record in the glaciated region of North America (e.g. the region covered by ice sheets during the Last Glacial Maximum (LGM)). Thus, few terrestrial records are available to provide information on the timing, onset and dynamics of the Laurentide Ice Sheet, the most extensive ice mass during the Late Pleistocene that covered ~80% of Canada during the LGM (Dyke et al.,

2002). Most extant deposits of Late Pleistocene age from formerly glaciated regions are found in the marginal areas of the former ice sheet(s) (e.g. Rémillard et al., 2013; Bajc et al., 2015; Rémillard et al., 2016) and thus offer limited constraint on the extent and dynamics of previous ice sheet(s), nor on the palaeoecology of more immediate periglacial settings.

The Hudson Bay Lowlands (HBL) are a vast low-lying peatland in central Canada bordered by the James and Hudson bays (Fig. 1). This region is presently one of North America's largest wetlands, consisting of bogs and fens with flora dominated by boreal (*Alnus*, *Betula*, *Larix*, *Picea*, *Salix*) and peatland taxa (Cyperaceae, Ericaceae, *Sphagnum*) (Riley, 2011). Holocene peat overlies a series of glacial and non-glacial deposits, including Pleistocene-aged sediments, which consist of multiple tills that are occasionally separated by *in situ* fluvial and organic-bearing sediments (known as the Missinaibi Formation; Skinner, 1973). The preservation of such extensive stratigraphic records near the center of the glaciated region makes the HBL critical for studying the history of the Late Pleistocene over North America (Dredge and Thorleifson, 1987; Kleman et al., 2010) because tills document the interaction between the northwest (Keewatin), and the northeast (Labrador) sectors of the former ice sheet (Fig. 1), whereas non-glacial materials (e.g. organic-bearing and fluvial sediments) yield insight into the timing and palaeoecology of ice-free intervals.

Several stratigraphic studies have taken place in the HBL, which have permitted the development of a Late Pleistocene stratigraphic framework for this region (Terasmae and Hughes, 1960; MacDonald, 1969; Skinner, 1973; Thorleifson et al., 1992; Thorleifson et al., 1993; Dubé-Loubert et al., 2013). Overall, this work has noted up to three tills below the Missinaibi Formation (Site 24M; Skinner, 1973) and two tills overlying this non-glacial interval (Dubé-Loubert et al., 2013). Despite these efforts, there remains uncertainty about the extent and

timing of glacial events in the HBL; mainly because correlation of glacial events over 1000+ km (e.g. the entire HBL region) is very difficult and glacial deposits are derived from different shifting ice centers. The Late Pleistocene record in the HBL is further complicated by the presence of multiple non-glacial events preserved in this region. Dating on some of the non-glacial sediments have yielded minimum age estimates (e.g. Stuiver et al., 1978; Mott and DiLabio, 1990); whereas others suggest that the non-glacial intervals may date to Marine Isotope Stage 5 (MIS 5; 130,000 to 71,000 yr BP; Allard et al., 2012; Dubé-Loubert et al., 2013) and MIS 7 (243,000 to 190,000 yr BP; Dubé-Loubert et al., 2013). There is also evidence that the region may have been ice-free during MIS 3 (57,000 to 29,000 yr BP; Andrews et al., 1983; Berger and Nielsen, 1990; Dalton et al., 2016). Increased study of glacial and non-glacial records in the HBL, including resolving the age of the Missinaibi Formation using chronology methods that span beyond the theoretical limits of radiocarbon dating, is critical to better interpret the dynamics of North American ice sheets during the Late Pleistocene.

Here, we present an analysis of the palaeoecology of a series of sub-till organic bearing deposits preserved at three riverbank exposures (informally named Sites 007, 008 and 009) along an 18-km stretch of the Albany River, HBL, Canada (51.9°N, 82.6°W; Fig. 1). These Albany sites were first documented by exploratory trips in the 1960s (Al-62, Al-63 and Al-65, respectively; Ontario Water Resources Commission, 1969). Each site contained organic-bearing non-glacial sediments that were intercalated between at least two diamicton units that were interpreted as till (glacial origin). Our primary aim was to constrain the timing of the non-glacial intervals at the Albany sites via optically stimulated luminescence (OSL) and radiocarbon dating, and to characterize the vegetation and palaeoenvironment during the non-glacial intervals using biological proxies (pollen, plant macrofossils) along with sedimentological data. Pollen-derived

palaeo-temperature and palaeo-precipitation reconstructions are also presented. We also present new data on the underlying and overlying glacial sediments to provide context for the interpretation of Late Pleistocene palaeoenvironments in the region. This was accomplished by examining lithology, geochemical composition, carbonate content and ice flow directional indicators of the diamicton units contained in the Albany sites. This research provides unique insight into glacial and non-glacial events at the innermost area of the glaciated region of North America that is complementary to other work in the region (Allard et al., 2012; Dubé-Loubert et al., 2013) as well as work in more peripheral regions (Rémillard et al., 2013; Bélanger et al., 2014; Bajc et al., 2015; Rémillard et al., 2016), and is similar to ongoing efforts to characterize ice-free intervals in the area of the Fennoscandian Ice Sheet in Northern Europe (Engels et al., 2008; Helmens and Engels, 2010; Helmens, 2014).

2. Methods

2.1. Fieldwork, sampling and geochronology

Fieldwork at the Albany sites was conducted by canoe during September 2014. Modern-day slump material was removed prior to making descriptions of each site and a representative sample was taken from each diamicton layer (above the zone of local incorporation near the base of each unit) for sedimentological and geochemical analyses. A single diamicton sample per unit is justified because previous work in this region has shown that diamictons display little sedimentological variation throughout the unit (e.g. Dubé-Loubert et al., 2013). Directional indicators (e.g. stone lines, boulder pavements and striations on the top of bullet-shaped boulders) were measured where observed in most diamicton layers using a geological compass (typically one to five measurements per layer). Samples were taken at 5-cm increments in the non-glacial interval for radiocarbon dating, loss on ignition (LOI), particle size analysis (PSA),

pollen and macrofossil analysis (Figs. 2–5). The only exception was at Site 009, where a steep slope restricted sampling to the bottom 2.7 m of the ~4-m non-glacial interval.

Age constraints on the non-glacial units were provided through OSL dating of quartz grains by the single aliquot regeneration protocol (Wintle and Murray, 2006) on selected, stratified, sand-bearing units at Site 007 (interpreted to be aeolian) and Site 008 (interpreted to be fluvial). Site 009 could not be dated via OSL because of a lack of suitable material for sampling (fluvial unit was too coarse-grained). Protocols for OSL dating are similar to those presented in Dalton et al. (2016). We limit the reporting of ages for those samples with at least 30 aliquots to determine an equivalent dose (Table 1; Fig. 6). The majority of aliquots (79 to 94%) were used to calculate an equivalent dose, with aliquots removed if (1) the recycling ratio was not between 0.90 and 1.10, (2) recuperation was >5%, (3) error in equivalent dose values was >10%, reflecting low light emissions (Demuro et al., 2013), and (4) if the 'fast ratio' was <20 (Durcan and Duller, 2011). Ultra-small aliquots were used for equivalent dose determination with a plate area of 1 mm^2 corresponding to about 20 to 40 grains per aliquot. Overdispersion analyses of equivalent dose populations were relatively low at 16 to 24% which indicates a single log-normal distribution, and thus the central age model was used in the final calculation of equivalent dose (Galbraith and Roberts, 2012). Water content of 25 ± 5% was estimated based on initial inferred conditions and subsequent glacial compaction of the sediment. Where appropriate, dose rate was adjusted for organic content by dilution based on loss on ignition values. The U, Th, Rb and K content was determined by inductively coupled plasma-mass spectrometry / optical emission spectroscopy (ICP-MS/OES) and these values, in combination with a calculated cosmic dose, were used to resolve a dose rate (Table 1; Fig. 6). Final OSL ages are presented in the Results section at 1-sigma error. However, errors are increased to 2-sigma ranges in the Discussion

(Section 4.5) to cover any variability introduced by uncertainty in moisture content, burial history, organic content and other errors (Mallinson et al., 2008; Schaetzl and Forman, 2008; Wood et al., 2010). Radiocarbon attempts on bulk organic material (peat) and wood from the non-glacial intervals at the Albany sites are reported in Table 2. These data are mostly from previous publications (MacDonald, 1969, 1971; Dalton et al., 2016), however two determinations at Site 008b are new (A. F. Bajc, Ontario Geological Survey, pers. comm., 2017).

2.2. Pollen, plant macrofossils and sedimentology

Pollen samples were processed using standard methods (Faegri and Iversen, 1975), plus density separation using sodium polytungstate to more effectively concentrate the pollen grains (Zabenskie, 2006). Identification of pollen grains followed Kapp et al. (2000), McAndrews et al. (1973) as well as reference collections held at the University of Toronto and the Royal Ontario Museum. Broken bisaccate pollen grains (*Pinus*, *Picea*) were rare, but when present, were counted if >50% of the grain was intact. A minimum of 150 pollen grains of herb, arboreal and shrub taxa were counted in each sample; taxa from these groups only were included in the pollen sum from which percentages were calculated. Samples that had <5000 grains/cm^3 based on the addition of a *Lycopodium* spike, or contained >10% broken/unidentified grains, were excluded from further analysis and are not reported here. A detrended correspondence analysis (DCA) plot of the fossil pollen assemblages was constructed using R package ‘vegan’ (Oksanen et al., 2015) and comprises all herb, arboreal and shrub pollen taxa. Stratigraphic plots were produced using R package ‘rioja’ (Juggins, 2015) and include all taxa which reach 1% abundance in at least one fossil sample per site.

Pollen-derived palaeoclimate reconstructions were developed using the modern analogue technique (Overpeck et al., 1985) and the North American Modern Pollen Database (n = 4833 sites; Whitmore et al., 2005) with additional sites from the HBL (n = 49; details on assembling this dataset are provided in Dalton et al., 2017). Only sites situated in the conifer/hardwood, boreal and forest-tundra biomes were included in the modern calibration set. Further, this calibration set was reduced to include only sites having pollen counts >150 grains, as well as those located in areas of <1200 mm of annual precipitation, resulting in a final calibration set of 1509 sites. The R package 'analogue' (Simpson, 2007; Simpson and Oksanen, 2014) using the k = 3 closest analogues and cross-validation (n = 500 bootstrap iterations) was used for pollen-based palaeoclimate reconstructions, where modern sites having a squared chord distance dissimilarity of <0.15 were taken to be analogues (Overpeck et al., 1985). Errors at each fossil site were based on the root mean squared error of prediction (RMSEP) of the modern calibration set using the k = 3 closest analogues. Modern-day values for the Albany sites were taken from gridded climate data as there were no local weather stations in the study area. Average summer temperature (June, July, August) at the Albany sites is ~14.2°C, while annual precipitation is ~564 mm (Natural Resources Canada, 2015).

Plant macrofossils, examined exclusively at Site 009, were concentrated by rinsing 15 cm^3 of organic-bearing sediment under a 100-µm sieve using water (occasionally overnight soaking in $Na_4P_2O_7$ solution was needed to disaggregate the sediment) and then identified under a stereomicroscope. Macrofossils provide direct evidence of local vegetation, and are thus important for validating and refining palaeoclimate reconstructions based solely on pollen data (Birks and Birks, 2000; Väliranta et al., 2009). Loss-on-ignition involved combustion of ~2 g (dry weight) of sediment at 550°C for 4 hours and then at 950°C for 2 hours to remove the

organic and carbonate fractions, respectively (Heiri et al., 2001). Sediment size distributions were determined using a Malvern Mastersizer 3000 and Hydro MV wet dispersion unit on samples that were first treated with H_2O_2 and HCl to remove organic and carbonate fractions.

2.3. Geochemical and sedimentology analyses on the diamicton layers

Geochemical data, particle size data, and the calcite-to-dolomite ratio (C:D) were used to characterize the diamictons, as well as to assess the degree to which they could be correlated among the three Albany sites. The carbonate content and the C:D ratio of each diamicton was determined using a Chittick apparatus (Dreimanis, 1962) on the <63 μm fraction, while particle size distributions were determined using sieves and a Microtrac particle size analyzer. Elemental data were measured by inductively coupled plasma atomic emission spectroscopy (ICP-AES) and inductively coupled plasma mass spectroscopy (ICP-MS) after digestion in aqua regia (Tables A1, A2). When measured values exceeded or fell below the instrument detection limit, 'greater than' values were assigned to 1.7x the detection limit and all 'less than' values were assigned to 0.55x the detection limit (Sanford et al., 1993). Elements were eliminated if replacements had to be made to more than 20% of the samples, which resulted in the removal of Be, Ca, K, Mg, Au, Pt, Se and Ta. If an element was measured in both ICP-AES and ICP-MS, only the latter values were retained because of the improved detection limits. Prior to statistical analysis, the centered log-ratio was taken in order to correct for any compositional bias in the data and to down-weight the influence of highly abundant elements (Aitchison, 1986; Grunsky, 2010). Geochemical data were visualized using Principal Component Analysis in R package 'vegan' (Oksanen et al., 2015), while cluster analysis was performed using the R base package using the 'average' agglomeration method (R Core Team, 2014). A similar multi-variate approach for characterizing diamicton units was used by McMartin et al. (2016). Consultation

with regional geological maps (Ontario Geological Survey, 2015) was used to suggest source area and possible glacier flow paths for the diamicton layers studied.

3. Results

3.1. Albany River Site 007

The lowermost exposed unit at Site 007 was a dark grey-brown diamicton (unit 1; Fig. 2A). It was massive to fissile, and consisted of a silt to sandy silt matrix with minor clay, pebbles, cobbles and boulders. Matrix particle size distribution was 38% sand, 45% silt and 17% clay (Fig. 7B). Unit 1 ranged from 2 to 11 m in thickness owing to a highly irregular contact with the overlying material. Rare stone lines along with isolated, faceted and striated boulders were contained in this diamicton; one stone line had striated tops of clasts between 190 and 232 °N.Az (based on 5 readings). A nearly continuous 30-cm thick layer of sand sub-divided unit 1 about 7 m above river level. This sand layer was truncated by the irregular contact with the sediments above (Fig 2A).

Overlying one part of the lowermost diamicton at Site 007 (unit 1) was a 1.8-m interval of brown to black, laminated, organic-bearing sediments (unit 2; Fig. 2A, also Fig. 2B, C) that consisted of silty clay (~35%), very fine sand and silt (~40%). These sediments were thinly interbedded and appeared to be deformed. This interval was generally less than 10% organic, with a 5–10% carbonate component (Fig. 2D). Radiocarbon dating of bulk peat from the 90-cm interval of this unit yielded a minimum limiting age of 42,700 ± 500 cal. yr BP (UOC-0597; Table 2). This bulk radiocarbon date is treated with caution due to the risk of contamination in a bulk sample containing carbon of mixed provenance (Dalton et al., 2016). Quartz grains yielded

an OSL age of 73,100 ± 6,365 yr BP (BG4227; Table 1; Fig. 6) at the same sampling interval as the radiocarbon age.

Overlying the organic-bearing interval was a light grey brown, massive, sandy-silt to silty-sand diamicton that contained granules, pebbles, cobbles and boulders (unit 3; Fig. 2A). Particle size analysis of the diamicton matrix contained 43% sand, 51% silt and 6% clay-sized particles (Fig. 7B). The diamicton ranged from 2 m (overlying the organic-bearing sediments) to 11 m in thickness where it was infilling a depression in the lower diamicton (unit 1). One boulder contained striations oriented at 204 °N. Az. Lenses and discontinuous layers of stratified sediments occur throughout this unit and rarely occur as 'u-shaped' stratified sediment bodies (predominantly sand, but also silt and clay laminate) in particular within the depression in unit 1. The upper surfaces of these 'u-shaped' bodies were planar, sharp and near-horizontal.

The uppermost diamicton at Site 007 was also light grey brown in colour and was characterized by massive sandy-silt to silty-sand with granules, pebbles, cobbles and boulders (unit 4; Fig. 2A). The matrix of the diamicton consisted of 32% sand, 57% silt and 11% clay; slightly finer-textured than the diamicton (unit 3) beneath (Fig. 2A; *see* Fig. 7B). Striations on the top of one faceted and striated boulder were oriented at 290 °N.az. Overlying this diamicton was a 2-m thick light brown, stratified, very fine sand and silt deposit that contained marine shells and shell fragments (unit 5). A thin, small pebble layer occurred at the base of this unit.

3.2. Albany River Site 008

The lowermost exposed unit at Site 008 was a dark grey-brown diamicton of 3 m thickness (unit 1; Fig. 3A), characterized as massive to fissile, consisting of a sandy silt to silty sand matrix with granules, pebbles, cobbles and boulders. Particle size analysis of the matrix

246 resulted in 36% sand, 53% silt and 11% clay (Fig. 7B). A faceted boulder had striations oriented
247 to 215 °N. Az. The upper surface of this diamicton gently sloped to the south (rightward on Fig.
248 3A). Two depressions in this diamicton's surface contained the thickest sequences of non-glacial
249 sediments; we identified the materials contained at the northern end as Site 008a, while those at
250 the southern end at a distance of ~50 m were Site 008b. The non-glacial sediments from Site
251 008a could be traced continuously along the exposure and were found to directly overlie the non-
252 glacial sediments of Site 008b, separated by a subtle, oxidized contact.

253 At the base of the non-glacial unit at Site 008a (Fig. 2B; field photograph) was a 35-cm
254 thick discontinuous band of stratified, fine and medium-grained sand and small pebble gravel.
255 Horizontal bedding and trough-crossbedding were noted in these sediments. Quartz grains from a
256 thin bed of very fine to fine grained sand in this unit yielded OSL ages of 59,120 ± 5,585 yr BP
257 and 59,695 ± 5,500 yr BP (BG4228 and BG4262; Table 1; Fig. 6). Overlying this sand deposit
258 was approximately 2 m of greasy organic-bearing silt, silty clay with rare thin layers and lenses
259 or small pebbly, medium to coarse sand, and layers of fine sand. The organic-bearing interval
260 contained ~25% sand, ~45% silt and ~30% clay, which varied throughout the unit, while the
261 organic component in this interval was 5–10%, with 5–8% carbonate (Fig. 3C). Radiocarbon
262 dating of bulk organic-bearing sediment from the 70-cm interval at site 008a suggested that it
263 was deposited at 45,500 ± 830 cal. yr BP (UOC-0594; Table 2).

264 At the southern end of the exposure, the non-glacial interval at Site 008b consisted of
265 brown to black organic matter, interbedded with very fine sand and silt. Overlying this dark
266 organic-bearing unit was a 20-cm interval of gravel, pebbly sand and fine sand, followed by ~4
267 m of rhythmically or interbedded fine sand, silt and silty clay with organic laminae (unit 2; Fig.
268 3A). Sand beds obtained thicknesses up to 15 cm and rhythmically bedded finer sediment

occurred in cycles of 1–2 cm. Quartz grains from a fine sand bed within the 20-cm interval of gravel, pebbly sand and fine sand yielded OSL ages of 72,640 ± 5,990 yr BP and 67,605 ± 5,765 yr BP (BG4263 and BG4264; Table 1; Fig. 6). Radiocarbon attempts on wood pieces at this site yielded >47,800 and >49,200 ^{14}C yr BP (ISGS-A3320 and ISGS-A3321; Table 2; A. F. Bajc, Ontario Geological Survey, pers. comm., 2017).

A dark grey brown diamicton of ~7 m thickness (unit 3; Fig. 3A) overlaid Site 008a and Site 008b. This diamicton was characterized by clayey silt with granules, pebbles, cobbles and some boulders. The particle size distribution of two matrix samples from this diamicton averaged 20% sand, 61% silt and 19% clay-sized particles (Fig. 7B). At the north end of Site 008a, this diamicton was massive, but numerous lenses and discontinuous layers of stratified sediment were present near the south of the exposure (Site 008b). At the south end of this exposure (Site 008b), an additional diamicton was present (unit 4). This light grey, massive diamicton was 4 m in thickness and consisted of sandy-silt to silty-sand with granules, pebbles, cobbles and boulders. The matrix contained 42% sand, 51% silt and 7% clay (Fig. 7B). Numerous sand and gravel lenses and layers were also present. The uppermost unit at Site 008 (unit 5) was 3 m of light brown, stratified, very fine sand, containing silt, small pebble and gravel layers/lenses and a thin gravel layer at the base. Marine shells were present in this unit.

3.3. Albany River Site 009

The lowermost exposed unit at Site 009 was a dark grey massive diamicton (unit 1; Fig. 4A), containing silty clay with granules and pebbles (12% sand, 52% silt and 36% clay; Fig. 7B). Striations on the top of one boulder were oriented to 340 °N.Az. Overlying this diamicton was a discontinuous layer (up to 30-cm thick) of brown, poorly-sorted pebble to small cobble gravel

(unit 2; also Fig. 4B, C), that was in turn overlain by 4 m of organic-bearing sediments (unit 3). The organic-bearing sediments were massive, laminated and consisted of clay silt and silt, with peaty layers. This unit was composed of ~35% clay, ~40% silt and the remainder as sand. The organic content was ~10–20%, and carbonate component ~2.5% (Fig. 4D). Radiocarbon attempts to date this bulk organic-bearing sediment all resulted in infinite determinations: >47,000, >48,800 and >54,000 ^{14}C yr BP (UOC-0595, UOC-0843, GSC-1185; Table 2).

Overlying the organic-bearing interval at Site 009 was a diamicton unit (unit 4; Fig. 4A). This diamicton was light grey-brown, loose, massive, and consisted of silty sand with granules, pebbles, cobbles and boulders. Matrix particle size consisted of 43% sand, 48% silt and 9% clay (Fig. 7B). Striations on one boulder were aligned to 170 °N.Az. The uppermost unit at this site was 3 m of light brown, stratified fine sand and silt with a thin small pebble gravel layer at the base (unit 5). This unit contained marine shells.

3.4. Correlation of diamicton units among the Albany sites

Principal Component Analysis of the trace element geochemistry along with particle size data and matrix carbonate content were used to group diamicton units. Cluster analysis of the elemental data suggested that diamicton units from the Albany sites can be divided into four groups (Fig. 7) that were separated along axis one of the PCA and accounted for 86% of the variance in the dataset. Till I, a group that contained only one sample (009-TM1), was characterized by the highest level of base metal elements of all the Albany sites, along with a relatively low calcite content (14.3%), extremely low dolomite content (0.1%), and a grain composition largely consisting of clay (47%) and silt (40%) with a small sand component. The lowermost diamicton units at Site 007 and 008 (007-TM1; 008-TM1, respectively) had similar

geochemistry, particle size distribution and matrix carbonate content (Fig. 7B), and thus comprised Till II. Till III was comprised of two samples from the same diamicton unit at Site 008 (008-TM2; 008-TM3) and had a geochemical signature suggesting intermediate levels of base metal elements as compared to Till I and Till II (Fig. 7A). The final group, Till IV, comprised the uppermost diamicton units at each site (007-TM3, 007-TM2, 009-TM2, 008-TM4). Total carbonate ranged from 35.6 to 39%, and the C:D ratio ranged from 0.6 to 1.4. Texturally, Till IV was characterized by a low clay component (<20%), silt comprised ~40%, and the remaining 40% was sand.

3.5. Biostratigraphy and palaeoclimate reconstructions at all Albany sites

The herb, arboreal and shrub components of the pollen assemblages at the Albany sites were very similar (Fig. 2D, 3C, 4D) and displayed little stratigraphic change through the organic-bearing intervals. Overall, *Picea* pollen dominated the assemblages with 53–55% of the average pollen count, followed by *Pinus* pollen at 19–23%, Poaceae at 8–9% and *Betula* at 6–9%. The remainder of the herbaceous, arboreal and shrub counts were dominated by *Salix* (2–3%), Asteraceae (1–2%), *Alnus* (~1%) and *Lycopodium* (~1%), along with <1% grains of *Abies*, Amaranthaceae, Caryophyllaceae, Cupressaceae, Ephedraceae, Ericaceae, Juglandaceae, Polygonaceae and Polypodiaceae. Wetland indicators (*Sphagnum* and Cyperaceae) were variable at each site, and generally ranged from 15–60% of the herb, arboreal and shrub pollen sum. Further, aquatic taxa *Equisetum* and *Pediastrum* were present at all three sites, with a few *Potamogeton* grains also present at Sites 007 and 008. Despite overall similarity among pollen at the fossil sites, subtle differences in the assemblages caused variability among sites in the ordination (Figure A1). For example, Site 007 had slightly more *Betula* (8.6%) and Site 009 overall had slightly higher *Pinus* (23.4%) than average values for the Albany sites. Temperate

taxa were also present rarely in the record, notably *Tsuga* (three grains at Site 008; five grains at Site 009) and *Quercus* (one grain at Site 009).

The majority of fossil intervals at the Albany sites (52 of 60 total examined samples) were suitable for quantitative palaeoclimate inferences owing to high pollen concentrations (e.g. >5000 grains/cm^3), well-preserved pollen grains (<10% broken/unidentified) and sufficient modern analogues (at least three modern sites having a squared chord distance dissimilarity of <0.15 with each fossil site). Of a possible 156 modern analogues (3 analogues used for each sample x 52 reconstructed intervals), 80 analogue sites (51%) were taken from the same three modern sites, one lying in the boreal forest of Central Canada, and two from the HBL. Pollen-based quantitative analysis from the organic-bearing interval at Site 007 yielded an average summer temperature of 13.3 ± 1.6°C (R^2 = 0.83, F = 7219, p < 0.001), which was marginally cooler, but given the errors, was indistinguishable from estimates for present-day obtained from a gridded climate dataset (14.2°C). Reconstructed annual precipitation at Site 007 was 635 ± 127 mm (R^2 = 0.83, F = 7472, p < 0.001), which may be slightly wetter, or the same as, estimated present-day values in this region (564 mm). Average summer temperature estimates for Site 008 and 009 were 14.1 ± 1.6°C (R^2 = 0.83, F = 7481, p < 0.001) and 14.6 ± 1.5°C (R^2 = 0.84, F = 7958, p < 0.001), respectively, while palaeo-precipitation estimates at these two sites were 620 ± 127 mm (R^2 = 0.83, F = 7447, p < 0.001) and 584 ± 122 mm (R^2 = 0.85, F = 8283, p < 0.001). Errors associated with these palaeoclimate reconstructions caused most estimates to overlap with present-day values at the Albany sites.

Macrofossils, examined only at Site 009, revealed more stratigraphic change than the pollen data (Fig. 5) and indicated a freshwater aquatic environment. Bryophytes were present throughout the examined record and were dominated by *Scorpidium* spp. Aquatic taxa were

similarly present throughout the record, notably, ephippia of *Daphnia* along with statoblasts of *Fredericella, Plumatella* and *Cristatella*. Leaf remains of *Potamogeton* and potentially *Najas* were also noted, although identification of the latter is tenuous. Overall, aquatic taxa became increasingly abundant in the upper part of the stratigraphy, between 180 and 270 cm. Seeds of herbaceous Caryophyllaceae, *Carex*, Poaceae, *Luzula* and *Typha* were present occasionally in the record, while Cyperaceae and *Equisetum* remains were also common. Remnants of *Betula* (bark, seeds), along with conifer bark and needles were present throughout. Charcoal and mites were also present, and showed a similar trend to the aquatic taxa, reaching highest abundances in the upper half of the sampling intervals (Fig. 5).

4. Discussion

We interpret diamicton units at each Albany site as subglacial till deposited by an actively flowing warm or wet-based glacier. This is based on the occurrence of striated and faceted clasts, bullet-shaped boulders, stone lines, boulder pavements and the overall massive appearance of the diamicton layers. Our correlation of till units, based on particle-size distribution, geochemistry (carbonate and trace element content), ice flow indicators and stratigraphic position allowed for the amalgamation of the three geographically-separated stratigraphic records along the Albany River, permitting some reconstruction of Late Pleistocene history at the center of the glaciated region. A composite stratigraphic plot for each of the Albany sites showing chronology results and till groupings is presented in Fig. 8.

4.1. Deposition of till at the Albany sites

The first event recorded at the Albany sites is the deposition of the tills underlying the non-glacial sediments (Fig. 8). The lowermost till layer at Site 009 (Till I) was deposited by ice

flowing toward the north-northwest, as indicated by stone lines and striated boulders. This flow direction helps to explain the low dolomite content of this till (Fig. 7B) because of the ice flow trajectory largely over limestone of the Moose River basin and the granitic Canadian Shield. A similar flow direction has been noted in the Rocksand till in the HBL attributed to MIS 5 (Thorleifson et al., 1992; 1993) or MIS 4 (ca. 71,000 to 57,000 yr BP; Kleman et al., 2010). In the Matagami area of central Québec, a northwest flow is the oldest one recorded (Veillette and Pomares, 1991; Veillette et al., 1999). Contrastingly, the lower till units at Site 007 and 008 (Till II) below the organic-bearing sediments were deposited by ice flowing toward the south-southwest, a trajectory over terrain underlain by Paleozoic limestone and dolomitic rocks, which is the cause of a high carbonate content in these units (Fig. 7B). Overall, the relative ages of Till I and Till II are not known; it is possible that they are the same age, representing different flow directions and shifting ice centers in the Matagami area (Parent et al., 1995; Veillette et al., 1999). Alternatively, they may have been deposited during different glacial advances prior to the non-glacial sediments.

4.2. Deposition of the non-glacial sediments at the Albany sites

The next event recorded at the Albany River Sites is the deposition of the non-glacial sediments (Fig. 8). At two of the Sites (008, 009), we interpret the non-glacial interval as a fluvial environment with the lowermost units representing channel or bar sediments of a river. The organic-bearing sediment fill was likely deposited upon river channel abandonment. This may have been an oxbow lake capable of supporting water-logged peatland biota. At Site 008, gravels, followed by rhythmically and interbedded sediments are interpreted to be the remnants of a channel bar with overlying bar-top sediments (overbank deposits). At Site 009, the poorly-sorted pebble and gravel unit is interpreted to be an active river channel lag deposit (gravel)

overlain by finer sediments on a bar top, or an infilled meander cutoff. An oxbow lake setting is supported by comparison to the stratigraphy and sedimentology of present-day oxbow lakes, which contain organic material interbedded with silts (Brooks, 2003; Brooks and Medioli, 2003), along with the presence of aquatic indicators in the pollen and macrofossil record (see Section 4.4). Variations in the sedimentological component may be the result of flooding of the nearby river, or from precipitation events. Channel bars, overbank deposits and meander scars are common features along the present-day Albany River. Thus, river morphology along with conditions controlling river gradient, discharge and sediment supply during these non-glacial intervals was likely similar to present-day conditions in the HBL.

Organic-bearing sediments at Site 007 overlie what we interpret to be a significant erosional event formed by either subglacial meltwater or fluvial activity. It is possible that this contact represents the river valley wall, thus the organic-bearing interval at this site may represent a tableland surface lying in the riparian region. This interpretation is supported by the higher relative elevation of this site compared to Site 008 and 009, along with increased *Betula* and *Sphagnum* pollen/spores, which could be expected given the closer proximity to wetlands as opposed to fluvial environments. In this case, sediment input may be from a combination of runoff and aeolian processes. Our interpretation of a palaeo-fluvial setting for the Albany sites aligns with the inferred setting of many other Pleistocene-aged sites in this region (e.g. Skinner, 1973; Dredge et al., 1990; Allard et al., 2012; Dubé-Loubert et al., 2013). Thus, it is possible that shelter from riverbanks aided in preserving many of the non-glacial Pleistocene records in this region (Barnett and Finkelstein, 2013).

4.3. Last Glacial Maximum (LGM), deglaciation and Holocene

Following the non-glacial episode was the deposition of Till III, a dark grey-brown unit that was preserved solely at Site 008 (Fig. 8). Geochemical analysis suggests that it may have been derived from a source area similar to Till I (009-TM1; ice flowing toward the northwest) owing to moderate base metal elements and a relatively high clay content (Fig. 5 and 7B). However, no flow indicators were observed. Till III is absent at Site 007 and 009, and may have been eroded, or in the case of Site 007, perhaps it did not extend that far west. The uppermost till layers at all three Albany sites were grouped as Till IV by PCA of the trace element content (Fig. 7A) and represent the most recent glacial events recorded at these sites. Directional indicators suggest that the lower Till IV at Site 007 and Till IV layers at the other two sites were deposited by a south-southwestward flowing glacier, supported by high dolomite content, suggesting prolonged transport over the dolostone-dominated Paleozoic terrain of the HBL (Ontario Geological Survey, 2015). Different ice-flow indicators from the uppermost till at Site 007 and its slightly finer texture suggest that ice flow was toward the west-northwest and may have resulted from a late local lobation of the ice margin, shift of the ice center, or may represent a distinct till unit and ice advance. We interpret the truncated "u"-shaped lenses of stratified sediment at Site 007 as Nye channels cut into existing sediment beneath actively moving ice by subglacial meltwater, suggesting that meltwater was abundant at the time of deposition of this unit. The presence of abundant water at the base of the glacier would also be conducive to shifting ice flow. The marine sediments overlying all three Albany sites are interpreted to be deposited by the Tyrell Sea in the Early Holocene (Lee, 1960).

The identification of possibly three tills above the Missinaibi Formation (the non-glacial interval) at the Albany sites is notable because it is somewhat at odds with the 'classic' HBL stratigraphy, which calls for two tills overlying this non-glacial interval (Thorleifson et al.,

1992). Thus, data from the Albany sites suggest the possibility of additional glacial events post-Missinaibi Formation not considered previously. A similar multiple-till pattern overlying the Missinaibi Formation is also present in other recent studies (Allard et al., 2012; Dubé-Loubert et al., 2013) however the correlation of these tills into the 'classical' stratigraphic framework remains largely unaddressed. The south-southwestward direction of ice movement in lower Till IV at Site 007 and at Site 008 and 009 is similar to reported ice flow directions of tills deposited in the Moose River Basin (Skinner, 1973), southern James Bay (Allard et al., 2012; Dubé-Loubert et al., 2013) and in the Matagami area (Veillette and Pomares, 1991) but direct correlation to any of these areas is not possible at this time, in part because it is very difficult to solely use ice flow direction (based on striations, fabrics and/or provenance) as a correlation tool within and between sub-glacial basins like those that occur in the HBL.

4.4. Interpretation of palaeoenvironments

The pollen assemblages at the Albany sites are similar to other Pleistocene records from the HBL that document boreal-peatland conditions (Terasmae and Hughes, 1960; Nielsen et al., 1986; Dredge et al., 1990; Allard et al., 2012; Dalton et al., 2017). The boreal interpretation is supported by the abundance of *Picea* and *Pinus* pollen along with tree-type *Betula* seeds and bark, conifer seed wings, bark, needles and charcoal at Site 009 (Fig. 5). The presence of *Betula* seeds and conifer seed wings indicate that climate conditions were favorable for pollination and seed development. The wetland interpretation is supported by aquatic, fen and forest macrofossil remains at Site 009 (Fig. 5), which suggest a minerogenic, paludified surrounding terrain with trees locally present. At all three Albany sites, the presence of *Pediastrum* and *Equisetum*, both aquatic indicators, corroborate sedimentological data which suggest that the organic-bearing intervals are shallow ponds or depressions on a flood plain (Figs. 2–4). Further, the presence of

Poaceae, along with occasional Asteraceae and other herb groups suggest that the canopy of the forested riparian region was occasionally open, and the palaeo-riverbanks may have supported *Salix*, *Alnus* and *Abies*. At Site 009, the increasing abundance of bryophytes, charcoal, sedge and aquatic remains between 180 and 270 cm (Fig. 5) corresponds to a transition toward layered and laminated sediments near the top of the section, thus we interpret a transition in local lacustrine conditions or perhaps increased erosion into the catchment.

All pollen-inferred palaeotemperatures (Figs. 2–4) overlap with present-day estimates for the region, but vary from slightly cooler (Site 007) to similar (Site 008) to slightly warmer (Site 009). The inclusion of rare temperate taxa (e.g. *Tsuga*, *Quercus*) in the pollen records at Site 008 and 009, along with the higher percentage of *Pinus* at Site 009, cause the slight temperature increase over what is inferred at Site 007. Temperate pollen grains are present in similar abundances in Holocene peat and lake cores from the HBL (McAndrews et al., 1982; O'Reilly et al., 2014), therefore it is possible that the organic-bearing sediments at the Albany sites were deposited when the temperate/boreal transition was in a similar position to today. The macrofossil record at Site 009 (Fig. 5) yielded few specific temperature indicators; while *Typha* is an indicator species in Finland following the 15.7°C July isotherm (Väliranta et al., 2015 and references therein), this taxon is present throughout modern and Holocene records in the HBL (Farley-Gill, 1980; Glaser et al., 2004; O'Reilly et al., 2014). Reconstructed precipitation at the Albany sites is similar or slightly higher compared to present-day, which may suggest that these sediments were deposited during MIS 5 as opposed to an interstadial (e.g. MIS 3), since palaeorecords dating to MIS 3 are thought to be characterized by less annual precipitation (see comparison of MIS 5 and MIS 3 palaeoenvironments presented in Dalton et al., 2017).

Most palaeoclimate studies using the North American Modern Pollen Database report R^2 values for temperature of ~0.9, and values of ~0.8 for precipitation (Fréchette and de Vernal, 2013; O'Reilly et al., 2014; Richerol et al., 2016). However both fall between 0.82 to 0.85 for the Albany sites, suggesting that annual precipitation may be better predicted at the Albany sites than other studies using the same calibration set. Errors reported for the palaeo-temperature and palaeo-precipitation reconstructions for the Albany sites are similar or less to what has previously been reported in Holocene and Pleistocene sites in the boreal region (Bunbury et al., 2012; O'Reilly et al., 2014; Richerol et al., 2016; Dalton et al., 2017). However, errors for most samples overlap with present-day values at the Albany sites, which places a limit on the inferences that can be made based on pollen data. Ordination of fossil pollen data (Figure A1) showed that the impact of rare temperate indicator taxa (e.g. *Tsuga*) was significantly minimized by the ubiquitous boreal taxa, thus adjusting the pollen sum (e.g. Gajewski, 2015) to down-weight the influence of boreal species may be critical for improving reconstructions in boreal environments. However, this was not possible at the Albany sites given the rarity of temperate taxa (few grains per interval) and the overwhelming abundance of boreal taxa in the pollen assemblage (>90%). An additional source of error is the accuracy of modern-day climate estimates for the HBL, which are interpolated from gridded datasets owing to a scarcity of weather stations.

4.5. Age of the non-glacial intervals preserved at the Albany sites

Age assignments for the non-glacial intervals at the Albany sites are complex. Firstly, we consider finite radiocarbon ages (UOC-0597, UOC-0594; Table 2) as ‘minimum ages’ because they are bulk peat dates where the carbon may have mixed provenance, and because of the lack of multiple finite ages at the same site (*see* Dalton et al., 2016). We consider the OSL ages to be

517 robust owing to the significant fast component (majority of aliquots retained for analysis), low
518 overdispersion values (all < 25%; Table 1; Fig. 6), reproducibility of ages at Site 008a and 008b,
519 and the fluvial setting that suggests sediments were well-bleached prior to deposition. Thus, the
520 OSL data suggest that the HBL, located at the innermost area of the glaciated region, was ice-
521 free and characterized by river systems and boreal peatlands at some point between ~86,000 and
522 ~48,000 yr BP (taking into account 2-sigma errors). However, the fall in global sea level during
523 MIS 4 suggests that the Laurentide Ice Sheet may have grown to near LGM extent during that
524 time (sea level -100 m below present-day; Grant et al., 2014), which would have glaciated the
525 HBL region. Thus the non-glacial interval(s) at the Albany sites very likely either pre- or post-
526 date the MIS 4 glacial event, and we present the following hypotheses: either all sites are late
527 MIS 5 (e.g. MIS 5a) or both MIS 5a and MIS 3 time intervals are present at the Albany sites.
528 Discussion on Site 009 is limited here since that site has no finite age estimates.

529 Taking into account the 2-sigma errors on the OSL dates, we suggest that the non-glacial
530 intervals at Site 007 and Site 008 both date to MIS 5a, a time when sea levels may have been
531 similar to present-day (Dorale et al., 2010; Creveling et al., 2017; Wainer et al., 2017), which
532 would most likely have left the HBL ice-free. This hypothesis is supported by pollen data at both
533 sites (007 and 008) which reflect vegetation similar in composition to present-day (Figs. 2-3),
534 consistent with a MIS 5 interpretation (Dalton et al., 2017). If the MIS 5a age assignment is
535 correct, the non-glacial interval at Site 007 and 008 may be contemporaneous with a non-glacial
536 interval preserved along the Nottaway River, southern James Bay, which has also been dated to
537 late-stage MIS 5 (via OSL and U-Th dating) and similarly contains palaeoecological indicators
538 (pollen, macrofossils) supporting climate conditions similar-to-present-day (Allard et al., 2012;
539 Dubé-Loubert et al., 2013). Comparison to other sites within the glaciated region is limited

because there are few sites that are both chronologically constrained to MIS 5a and contain palaeoecological data, specifically pollen. However, outside of the HBL, another site from Eastern Canada that has been constrained to MIS 5a via U-Th dating also suggests that climate was similar to present-day at that time (de Vernal et al., 1986).

It is possible that two different non-glacial intervals are present at Site 008. Large errors on the OSL ages, particularly when considered at 2-sigma range, allow the non-glacial interval at Site 008a to be placed into early MIS 3 (e.g. 57,000 to 48,000 yr BP), an ice-limited interval which is supported by other sites in the HBL (Dalton et al., 2016; 2017) as well as emerging sea level and geophysical estimates (Pico et al., 2016; 2017) that support significantly reduced ice cover over some part of the eastern sector of the Laurentide Ice Sheet during that time. Sediments from Site 008a stratigraphically overlie Site 008b, and are separated by a subtle contact, thus it is possible that both MIS 5a (008b) and MIS 3 (008a) sediments are present at the same site. However, additional geochronology work is needed to test this hypothesis. If correct, a MIS 3 age assignment for Site 008a may be supported by a finite radiocarbon age at that site (UOC-0594; 45,500 ± 830 cal. yr BP), and Site 008 may be one of the first documented sites in the HBL which contains organic bearing sediments from more than one non-glacial interval.

5. Conclusions

The Laurentide Ice Sheet was the predominant North American ice mass at the LGM, however there is limited terrestrial data to delineate its pre-LGM palaeogeography or dynamics owing to extensive erosion of the stratigraphic record in the formerly glaciated region. Our study of three stratigraphic records from the HBL, located at the geographic center of the glaciated region, provided information about the timing, inception and direction of North American ice

growth and documented at least four ice advances from the eastern (Labrador) sector of the Laurentide Ice Sheet over the region. At the Albany sites, the close proximity (within 18 km) of tills of differing ice flow directions and from different source areas, at similar stratigraphic positions (both above and below non-glacial sediments), may indicate that deposition of these tills occurred near the ice-margin. Intercalated between glacial deposits at the Albany sites were organic-bearing sediments that suggested ice-free conditions at the innermost area of the glaciated region. Biostratigraphic (pollen, macrofossils) and sedimentological work suggested the development of a landscape similar to present-day conditions during these non-glacial intervals; a northern boreal peatland containing vegetation (*Picea*, *Pinus*, Poaceae, *Betula*, Cyperaceae, *Sphagnum*) and climate (precipitation and temperature) analogous to present-day, whereas fluvial deposits suggested the development of palaeo-river systems of analogous morphology, discharge and sediment supply compared to present-day. The development of these landscapes was only possible if the HBL, lying at the geographic center of the glaciated region, was ice-free. Chronology data suggested that these non-glacial events occurred at some point between ~86,000 and 48,000 yr BP. Available chronology and palaeoecological data support an MIS 5a assignment for the Albany sites, however the possibility remains that later intervals (e.g. MIS 4 and MIS 3) may be represented here, thus signaling a large-scale recession of the Laurentide Ice Sheet during the last glacial cycle. Assuming that the Laurentide Ice Sheet was the dominant ice mass during that time, results from this research represent important empirical data for testing models of ice sheet volume/dynamics as well as refining estimates of global sea level during the Late Pleistocene.

Acknowledgments

584 This research was supported by funding from the Natural Sciences and Engineering
585 Research Council of Canada (NSERC) to S.A.F; the University of Toronto Centre for Global
586 Change Science, Ontario Graduate Scholarship and Northern Scientific Training Program to
587 A.S.D; and the Ontario Geological Survey. We are grateful to S. Williams and Missinaibi
588 Headwaters Outfitters for fieldwork assistance; J. Davison, A. Soleski and T. Hui for laboratory
589 assistance; J. Desloges for the use of the Malvern Mastersizer 3000 and Hydro MV wet
590 dispersion unit. Some of the modern pollen data used in the calibration set were obtained from
591 the Neotoma Paleoecology Database (http://www.neotomadb.org), and the work of the data
592 contributors and the Neotoma community is gratefully acknowledged. We also thank Andy Bajc
593 for sharing radiocarbon data, Karin Helmens for discussions, and two anonymous reviewers for
594 helpful comments.

595

596 **Table 1.** Optically stimulated luminescence (OSL) ages on quartz grains from the Albany sites, the Hudson Bay Lowlands, Canada.

Field #	Lab number	Aliquots[a]	Grain Size (μm)	Equivalent dose (Gray)[b]	Over-dispersion (%)[c]	U (ppm)[d]	Th (ppm)[d]	K (%)[d]	H_20 (%)	Cosmic Dose rate (mGray/yr)	Dose rate (mGray/yr)	OSL age (yr)[h] (1-sigma error)	OSL age (yr) (2-sigma error)
Site 007	BG4227	31/35	150-250	131.83 ± 6.17	16 ± 2	1.07 ± 0.01	4.40 ± 0.01	1.78 ± 0.01	25 ± 5	0.12 ± 0.01	1.80 ± 0.09[g]	73,100 ± 6365	73,100 ± 12,730
Site 008a	BG4228	38/48	150-250	81.57 ± 4.43	24 ± 3	0.80 ± 0.01	2.77 ± 0.01	1.41 ± 0.01	25 ± 5	0.06 ± 0.006	1.38 ± 0.07	59,120 ± 5585	59,120 ± 11,170
Site 008a	BG4262	30/32	150-250	87.97 ± 4.87	21 ± 3	1.03 ± 0.01	4.33 ± 0.01	1.36 ± 0.01	25 ± 5	0.05 ± 0.005	1.47 ± 0.08	59,695 ± 5500	59,695 ± 11,000
Site 008b	BG4263	40/48	150-250	125.25 ± 5.60	19 ± 2	1.68 ± 0.01	4.34 ± 0.01	1.55 ± 0.01	25 ± 5	0.05 ± 0.005	1.72 ± 0.09	72,640 ± 5990	72,640 ± 11,980
Site 008b	BG4264	42/52	150-250	134.72 ± 6.45	20 ± 2	2.18 ± 0.01	6.22 ± 0.01	1.64 ± 0.01	25 ± 5	0.05 ± 0.005	1.99 ± 0.10	67,605 ± 5765	67,605 ± 11,530

597
598 [a]Aliquots used in equivalent dose calculations versus original aliquots measured.
599 [b]Equivalent dose calculated on a pure quartz fraction with about 20-40 grains/aliquot and analyzed under blue-light excitation (470 ± 20 nm)
600 by single aliquot regeneration protocols (Murray and Wintle, 2003). The central age model of Galbraith et al. (1999) was used to calculated equivalent dose when overdispersion
601 values are <25% (at one sigma errors; a finite mixture or minimum age model was used with overdispersion values >20% to determine the youngest equivalent dose population.
602 [c]Values reflects precision beyond instrumental errors; values of ≤ 25% (at 1 sigma limit) indicate low dispersion in equivalent dose values and an unimodal distribution.
603 [d]U, Th and K content analyzed by inductively-coupled plasma-mass spectrometry analyzed by ALS Laboratories, Reno, NV; U content includes Rb equivalent.
604 includes also a cosmic dose rate calculated from parameters in Prescott and Hutton (1994).
605 [f]Assumes an organic content of 25 ± 5% derived from lost on ignition values.
606 [g]Assumes an organic content of 2 ± 1%
607 [h]Systematic and random errors calculated in a quadrature at one standard deviation. Datum year is AD 2010

608 **Table 2.** Radiocarbon age determinations from Albany Sites 007, 008 and 009.

609

Site	Interval	Lab Code	Dated material	^{14}C age (yr BP)	Calibrated yr BP (2-sigma error)[a]	Publication
007	90-cm	UOC-0597	peat	38,829 ± 350	42,700 ± 500	Dalton et al. (2016)
008a	70-cm	UOC-0594	peat	42,146 ± 458	45,500 ± 830	Dalton et al. (2016)
008b		ISGS-A3320	wood	> 47,800	n/a	A. F. Bajc (Ontario Geological Survey), pers. comm., 2017
008b		ISGS-A3321	wood	> 49,200	n/a	A. F. Bajc (Ontario Geological Survey), pers. comm., 2017
009	55-cm	UOC-0595	peat	> 47,000	n/a	Dalton et al. (2016)
009	55-cm	UOC-0843	peat	> 48,800	n/a	Dalton et al. (2016)
009		GSC-1185	peat	> 54,000	n/a	MacDonald (1969, 1971)

610

611 [a]Ages were calibrated using CALIB Rev 7.0.4 and the 2013 radiocarbon calibration curve (Stuiver and Reimer, 1993; Reimer et
612 al., 2013)

613
614

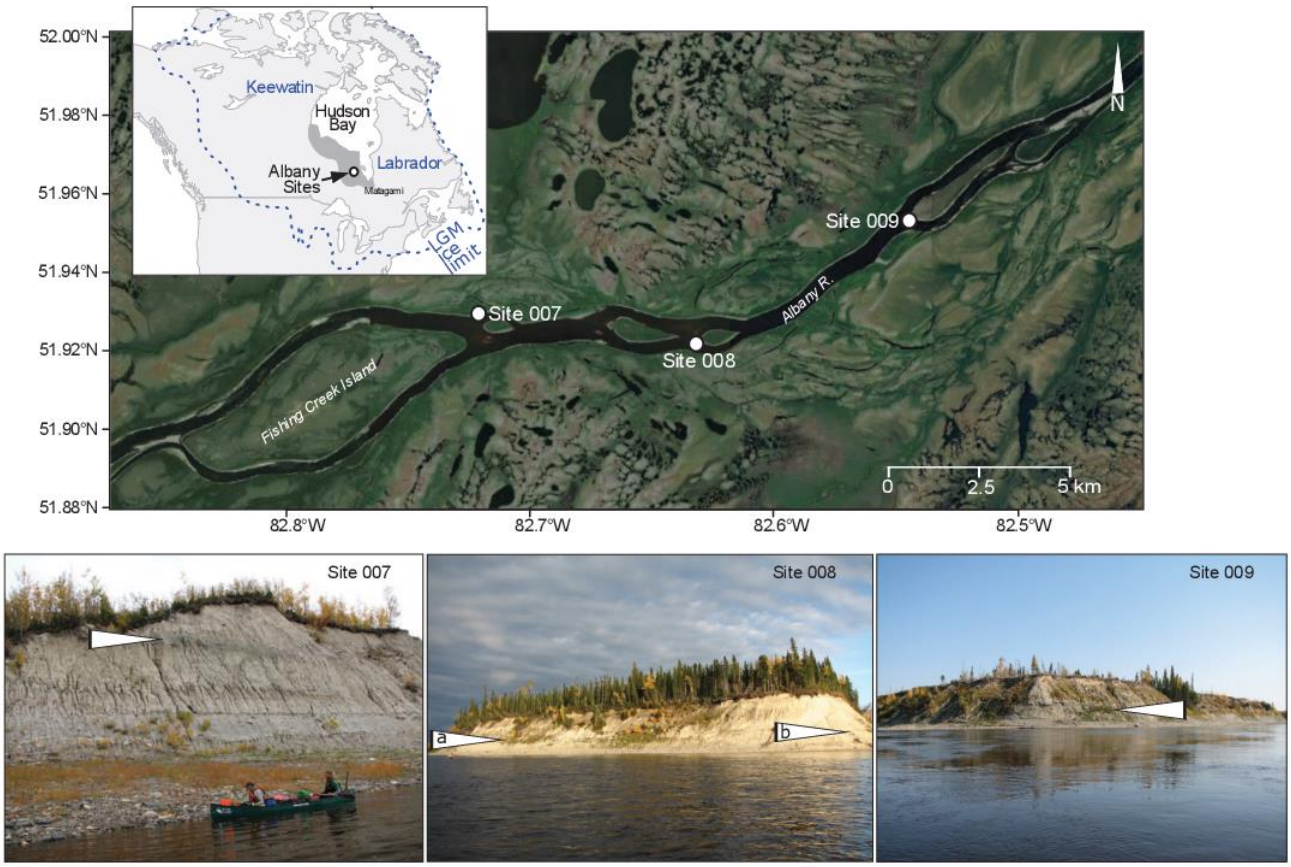

615

616 **Fig. 1.** Map of Albany River sites and photographs. Satellite imagery is from Google Earth. Inset
617 map situates the study area within North America and shows the HBL (shaded area), the LGM
618 extent of the Laurentide Ice Sheet (hatched blue line) and the location of the Keewatin and
619 Labrador sectors. Arrows on each field photograph show the location of the organic-bearing
620 interval.

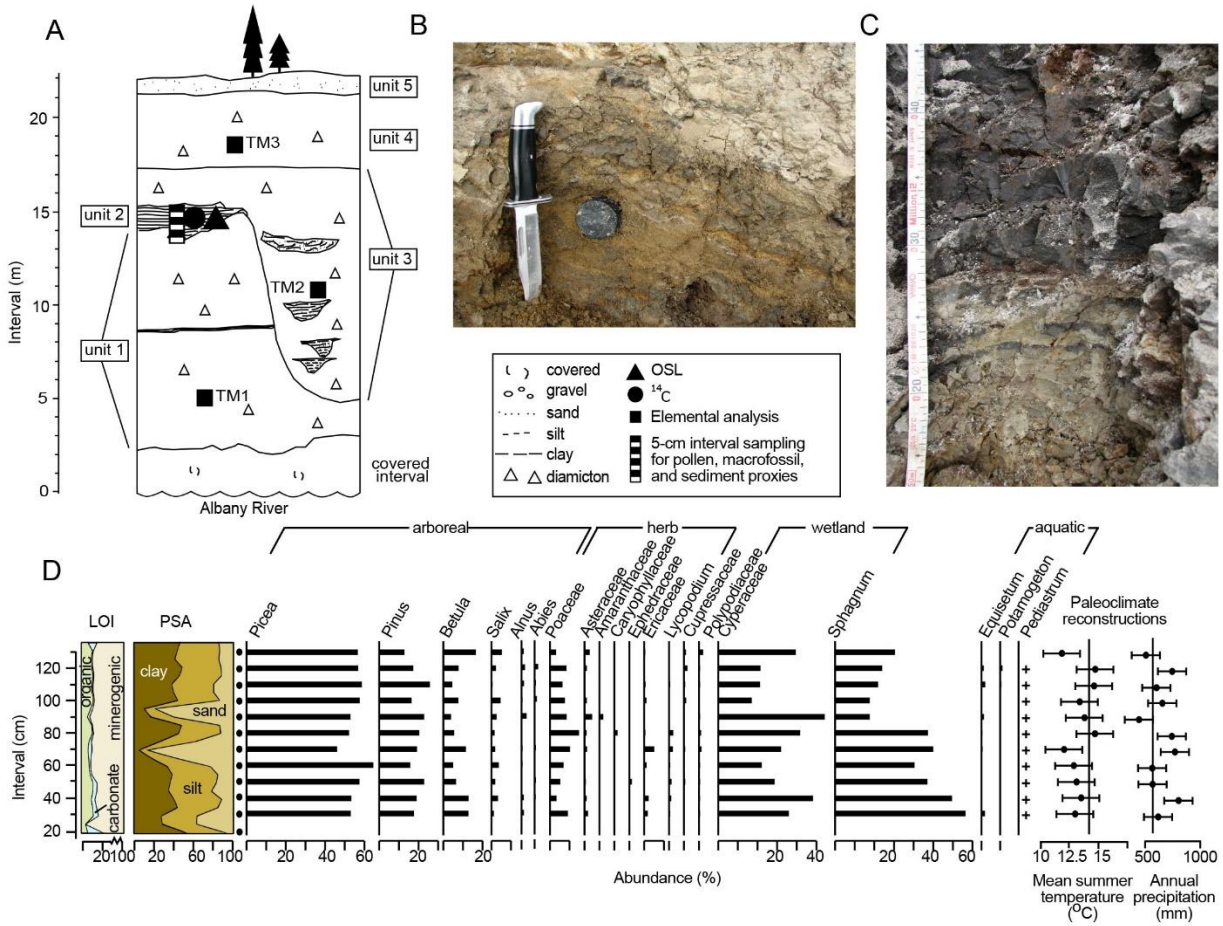

621

622 **Fig. 2.** Stratigraphy and pollen data for Site 007. A: sketch of section and locations of samples.
623 B: photograph showing OSL sample location and surrounding sediment. C: base of the non-
624 glacial interval showing the transition from sand-rich (light colours) sediments to silt- and clay-
625 rich organic sediments (darker colours). Note the intervals of interbedded/deformed silty clay,
626 very fine sand and silt. D: biostratigraphic data from the non-glacial interval at Site 007,
627 including LOI and PSA. Pollen samples were examined every 10 cm (indicated by the filled
628 circles adjacent to the PSA data); missing pollen data indicate an interval of poor preservation.
629 All arboreal, herb and shrub taxa reaching 1% in at least one sample are shown here, in addition
630 to all wetland and aquatic indicators. Vertical lines in the palaeoclimate reconstructions represent
631 estimates for present-day.

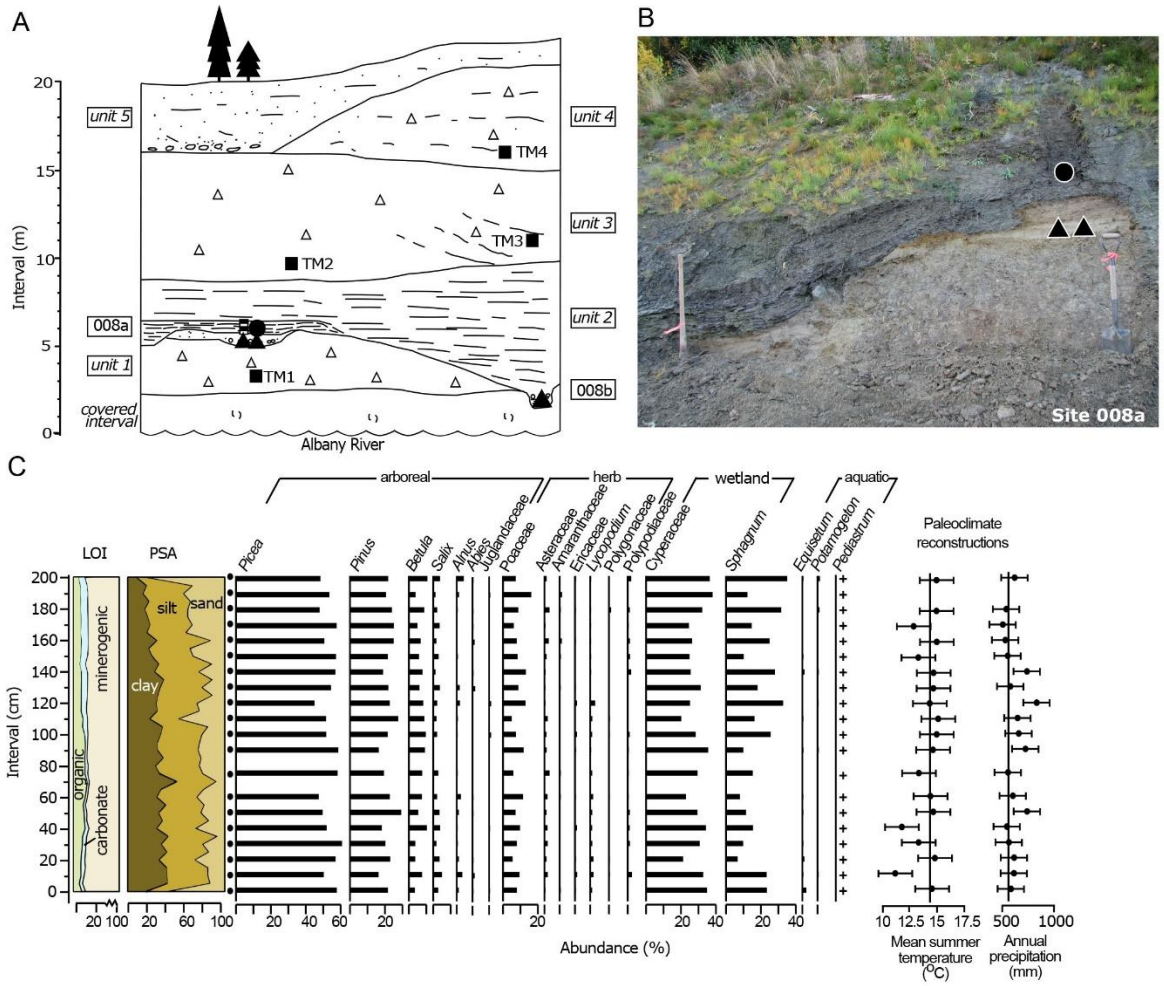

Fig. 3. Stratigraphy and pollen data for Site 008. A: sketch of section and locations of samples. B: photograph showing the organic-bearing sediments at Site 008a along with OSL and radiocarbon sample locations. C: biostratigraphic data from the non-glacial interval at Site 008, including LOI and PSA. See caption in Fig. 4-2 for further details on the stratigraphic legend and biostratigraphy plot.

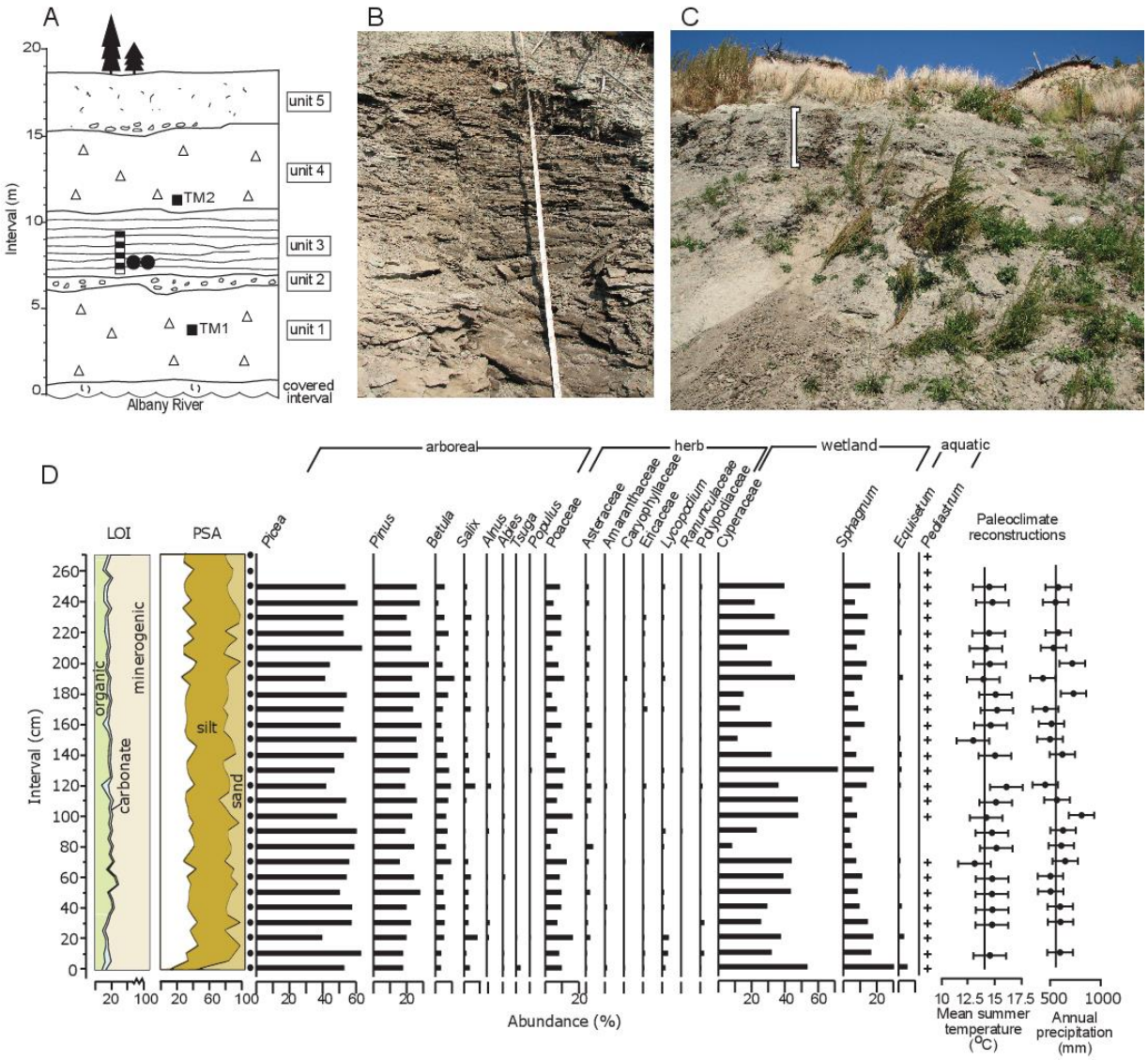

638

639 **Fig. 4.** Stratigraphy and pollen data for Site 009. A: sketch of section and locations of samples;
640 B: photograph showing sediments from the non-glacial interval. C: photograph taken from the
641 base of Site 009 showing the location of the organic-bearing unit (indicated by bracket). D:
642 biostratigraphic data from the non-glacial interval at Site 009, including LOI and PSA.

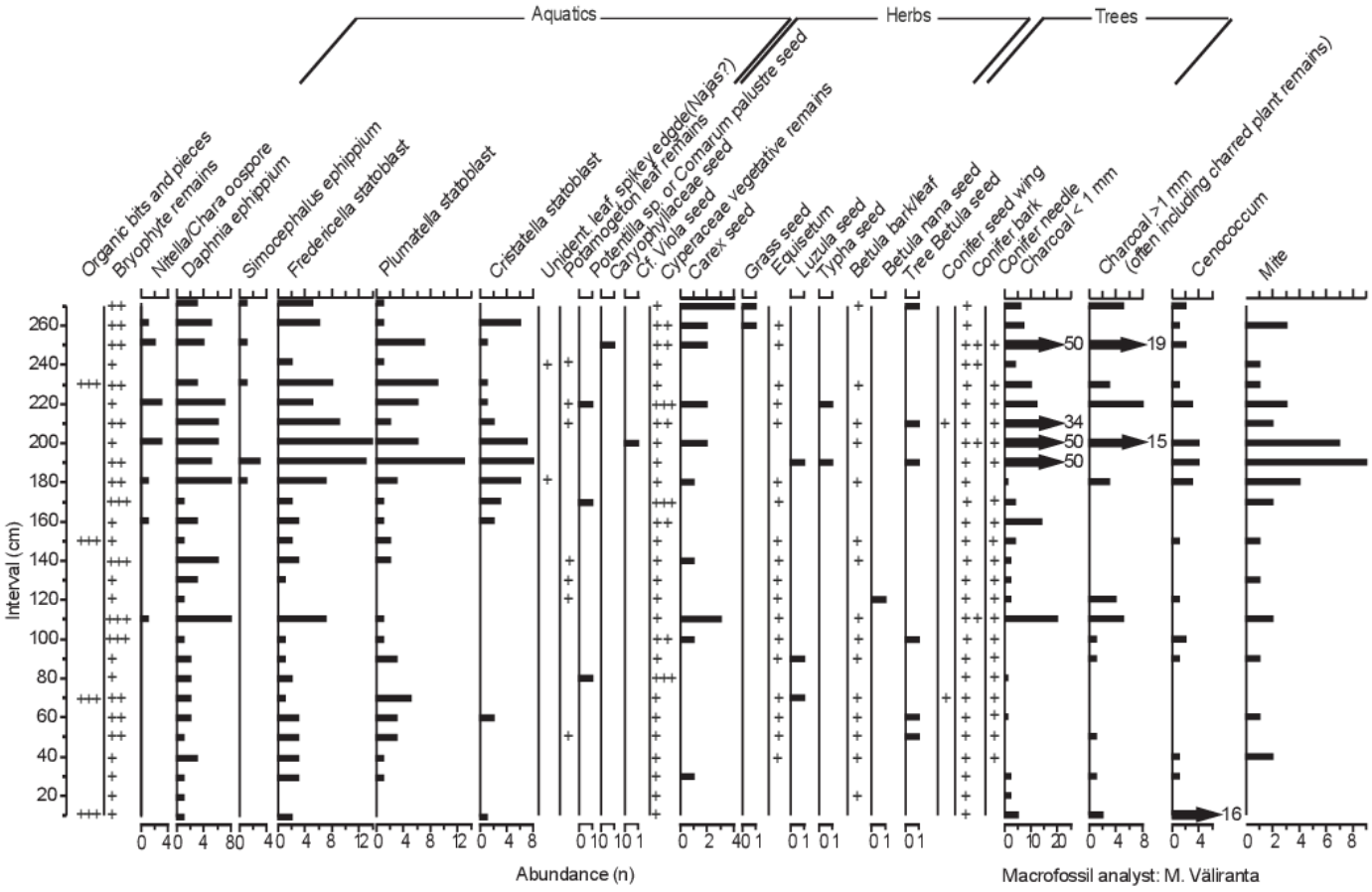

643 **Fig. 5.** Macrofossil data for Site 009. Most data are presented in raw counts; however, some taxa
644 are qualitatively described as present (+), frequent (++) and abundant (+++). Bryophytes consist
645 mainly of *Scorpidium* spp, but fen species are nearly continuously present, including
646 *Aulacomnium palustre*, *Cinclidium stygium/Rhizomnium* sp., *Meesia triquetra*, and
647 *Tomentypnum nitens.*
648

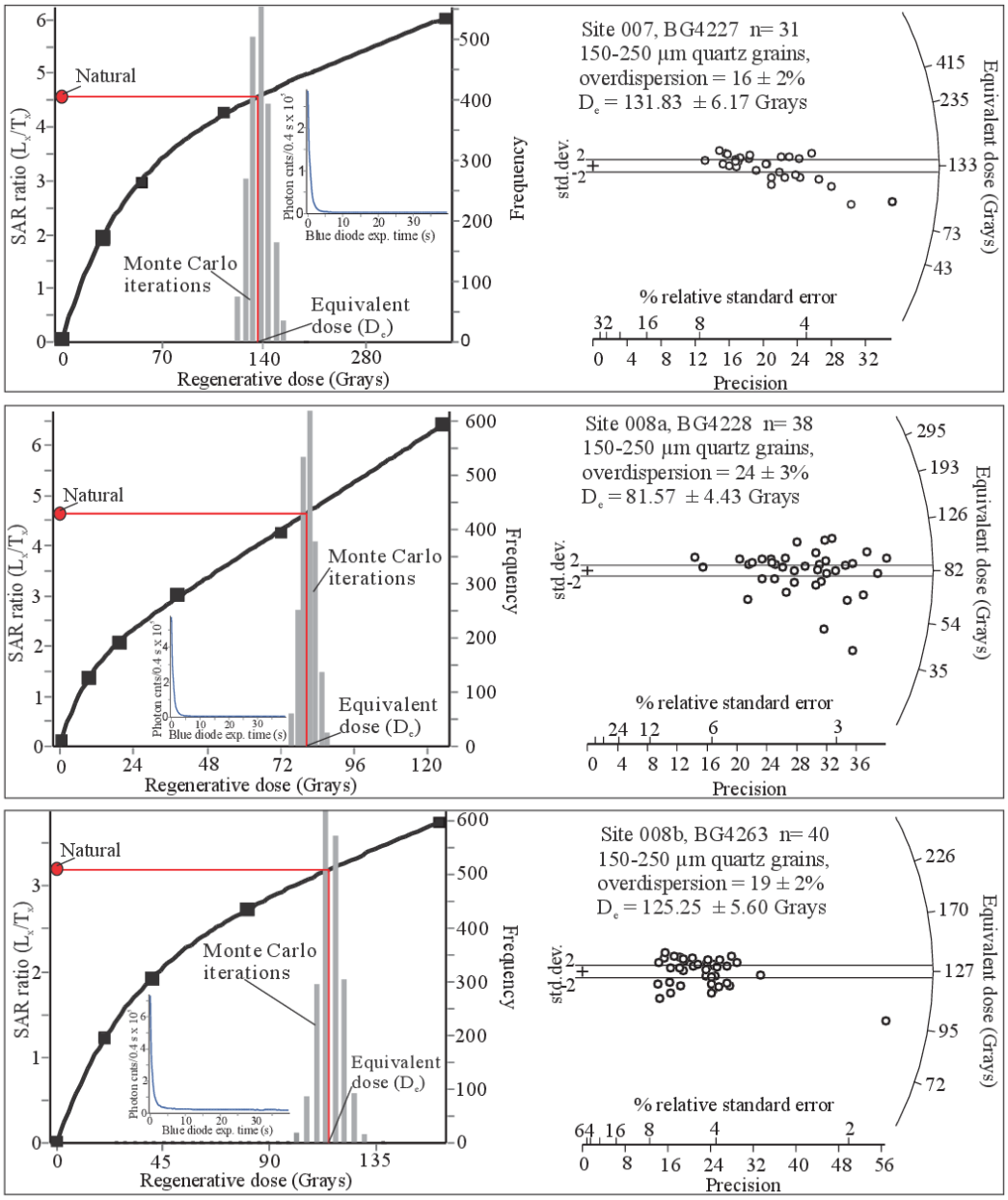

649

650 **Fig. 6.** Single aliquot regenerative (SAR) dose response curve, with inset figure showing
651 representative shine down curve, and adjacent figure a radial plot of equivalent dose values for
652 samples BG4227, BG4228 and BG4263.

653

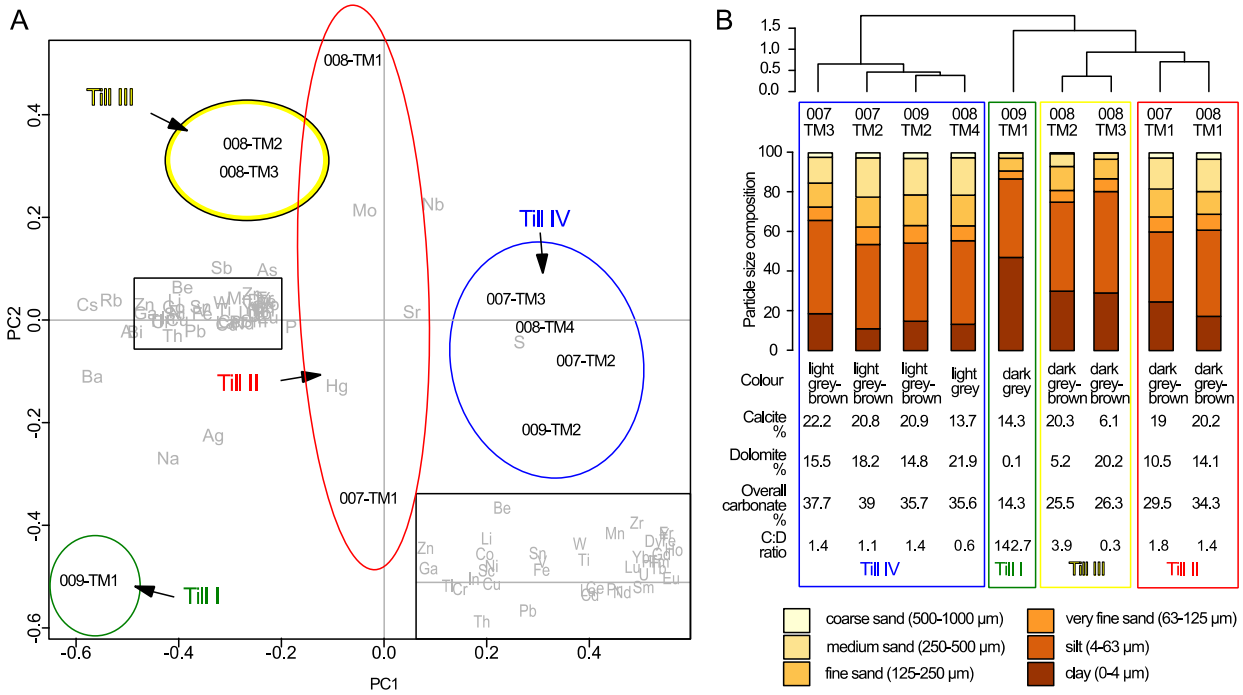

654

655 **Fig. 7**. Results of till elemental analysis and sedimentology of the diamicton units at the Albany
656 sites. A: Ordination by PCA of samples by elemental data. All till samples (black text) and
657 elements (grey text) are plotted in the ordination space. B: Sediment size distribution, colour
658 descriptions and carbonate determinations for each sample, showing cluster analysis groups that
659 were derived from the elemental data.

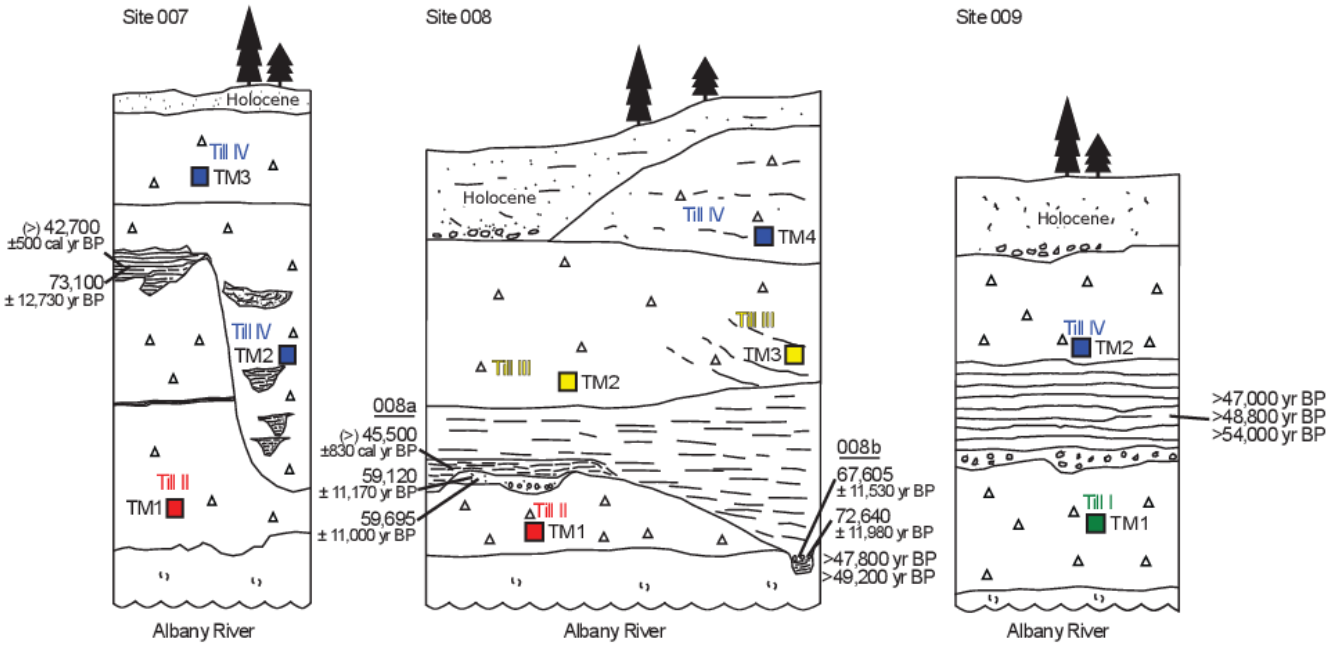

660

661 **Fig. 8.** Composite stratigraphic plot showing sample locations, chronology and till groupings at
662 the Albany sites. Finite radiocarbon ages at Site 007 and 008 are shown here as minimum ages
663 and OSL data are presented with 2-sigma errors (see text for details). Sites are located along an
664 18-km stretch of the Albany River.

665

References

Aitchison, J., 1986. The Statistical Analysis of Compositional Data. Chapman & Hall, New York.

Allard, G., Roy, M., Ghaleb, B., Richard, P.J.H., Larouche, A.C., Veillette, J.J., Parent, M., 2012. Constraining the age of the last interglacial–glacial transition in the Hudson Bay lowlands (Canada) using U–Th dating of buried wood. Quaternary Geochronology 7, 37-47.

Andrews, J.T., Shilts, W.W., Miller, G.H., 1983. Multiple deglaciations of the Hudson Bay Lowlands, since deposition of the Missinaibi (Last-Interglacial?) Formation. Quaternary Research 19, 18-37.

Bajc, A.F., Karrow, P.F., Yansa, C.H., Curry, B.B., Nekola, J.C., Seymour, K.L., Mackie, G.L., 2015. Geology and paleoecology of a Middle Wisconsin fossil occurrence in Zorra Township, southwestern Ontario, Canada. Canadian Journal of Earth Sciences 52, 386-404.

Barnett, P.J., Finkelstein, S.A., 2013. Sub-till organic-bearing sediments of the Hudson Bay Lowland: stratigraphy and geochronology, CANQUA-CGRG Conference 2013, Edmonton, Alberta, p. 53.

Bélanger, N., Carcaillet, C., Padbury, G.A., Harvey-Schafer, A.N., Van Rees, K.J., 2014. Periglacial fires and trees in a continental setting of Central Canada, Upper Pleistocene. Geobiology 12, 109-118.

Berger, G.W., Nielsen, E., 1990. Evidence from thermoluminescence dating for Middle Wisconsinan deglaciation in the Hudson Bay Lowland of Manitoba. Canadian Journal of Earth Sciences 28, 240-249.

689 Birks, H.H., Birks, H.J.B., 2000. Future uses of pollen analysis must include plant macrofossils.
690 Journal of Biogeography 27, 31-35.
691 Brooks, G.R., 2003. Alluvial deposits of a mud-dominated stream: the Red River, Manitoba,
692 Canada. Sedimentology 50, 441-458.
693 Brooks, G.R., Medioli, B.E., 2003. Deposits and Cutoff Ages of Horseshoe and Marion Oxbow
694 Lakes, Red River, Manitoba. Géographie physique et Quaternaire 57, 151-158.
695 Brovkin, V., Brücher, T., Kleinen, T., Zaehle, S., Joos, F., Roth, R., Spahni, R., Schmitt, J.,
696 Fischer, H., Leuenberger, M., Stone, E.J., Ridgwell, A., Chappellaz, J., Kehrwald, N.,
697 Barbante, C., Blunier, T., Dahl Jensen, D., 2016. Comparative carbon cycle dynamics of
698 the present and last interglacial. Quaternary Science Reviews 137, 15-32.
699 Bunbury, J., Finkelstein, S.A., Bollmann, J., 2012. Holocene hydro-climatic change and effects
700 on carbon accumulation inferred from a peat bog in the Attawapiskat River watershed,
701 Hudson Bay Lowlands, Canada. Quaternary Research 78, 275-284.
702 Creveling, J.R., Mitrovica, J.X., Clark, P.U., Waelbroeck, C., Pico, T., 2017. Predicted bounds
703 on peak global mean sea level during marine isotope stages 5a and 5c. Quaternary
704 Science Reviews 163, 193-208.
705 Dalton, A.S., Finkelstein, S.A., Barnett, P.J., Forman, S.L., 2016. Constraining the Late
706 Pleistocene history of the Laurentide Ice Sheet by dating the Missinaibi Formation,
707 Hudson Bay Lowlands, Canada. Quaternary Science Reviews 146, 288-299.
708 Dalton, A.S., Väliranta, M., Barnett, P.J., Finkelstein, S.A., 2017. Pollen and macrofossil-
709 inferred paleoclimate at the Ridge Site, Hudson Bay Lowlands, Canada: Evidence for a
710 dry climate and significant recession of the Laurentide Ice Sheet during Marine Isotope
711 Stage 3. Boreas 46, 388-401.

712 de Vernal, A., Causse, C., Hillaire-Marcel, C., Mott, R., Occhietti, S., 1986. Palynostratigraphy
713 and Th/U ages of upper Pleistocene interglacial and interstadial deposits on Cape Breton
714 Island, eastern Canada. Geology 14, 554-557.
715 Demuro, M., Arnold, L.J., Froese, D.G., Roberts, R.G., 2013. OSL dating of loess deposits
716 bracketing Sheep Creek tephra beds, northwest Canada: Dim and problematic single-
717 grain OSL characteristics and their effect on multi-grain age estimates. Quaternary
718 Geochronology 15, 67-87.
719 Dorale, J.A., Onac, B.P., Fornós, J.J., Ginés, J., Ginés, A., Tuccimei, P., Peate, D.W., 2010. Sea-
720 Level Highstand 81,000 Years Ago in Mallorca. Science 327, 860-863.
721 Dredge, L.A., Morgan, A.V., Nielsen, E., 1990. Sangamon and Pre-Sangamon Interglaciations in
722 the Hudson Bay Lowlands of Manitoba. Géographie physique et Quaternaire 44, 319-
723 336.
724 Dredge, L.A., Thorleifson, L.H., 1987. The Middle Wisconsinan History of the Laurentide Ice
725 Sheet. Géographie physique et Quaternaire 41, 215-235.
726 Dreimanis, A., 1962. Quantitative gasometric determination of calcite and dolomite by using
727 Chittick apparatus. Journal of Sedimentary Research 32, 520-529.
728 Dubé-Loubert, H., Roy, M., Allard, G., Lamothe, M., Veillette, J.J., 2013. Glacial and nonglacial
729 events in the eastern James Bay lowlands, Canada. Canadian Journal of Earth Sciences
730 50, 379-396.
731 Durcan, J.A., Duller, G.A.T., 2011. The fast ratio: A rapid measure for testing the dominance of
732 the fast component in the initial OSL signal from quartz. Radiation Measurements 46,
733 1065-1072.

734 Dyke, A.S., Andrews, J.T., Clark, P.U., England, J.H., Miller, G.H., Shaw, J., Veillette, J.J.,
735 2002. The Laurentide and Innuitian ice sheets during the Last Glacial Maximum.
736 Quaternary Science Reviews 21, 9-31.
737 Engels, S., Bohncke, S.J.P., Bos, J.A.A., Brooks, S.J., Heiri, O., Helmens, K.F., 2008.
738 Chironomid-based palaeotemperature estimates for northeast Finland during Oxygen
739 Isotope Stage 3. Journal of Paleolimnology 40, 49-61.
740 Faegri, K., Iversen, J., 1975. Text Book of Pollen Analysis, 3rd Edition ed. Munksgaard,
741 Copenhagen and Denmark.
742 Farley-Gill, L.D., 1980. Contemporary pollen spectra in the James Bay Lowland, Canada, and
743 comparison with other forest-tundra assemblages. Géographie physique et Quaternaire
744 34, 321-334.
745 Fréchette, B., de Vernal, A., 2013. Evidence for large-amplitude biome and climate changes in
746 Atlantic Canada during the last interglacial and mid-Wisconsinan periods. Quaternary
747 Research 79, 242-255.
748 Gajewski, K., 2015. Quantitative reconstruction of Holocene temperatures across the Canadian
749 Arctic and Greenland. Global and Planetary Change 128, 14-23.
750 Galbraith, R.F., Roberts, R.G., 2012. Statistical aspects of equivalent dose and error calculation
751 and display in OSL dating: An overview and some recommendations. Quaternary
752 Geochronology 11, 1-27.
753 Galbraith, R.F., Roberts, R.G., Laslett, G.M., Yoshida, H., Olley, J.M., 1999. Optical dating of
754 single and multiple grains of quartz from Jinmium rock shelter, northern Australia: Part I,
755 Experimental design and statistical models. Archaeometry 41, 339-364.

Glaser, P.H., Hansen, B.C.S., Siegel, D.I., Reeve, A.S., Morin, P.J., 2004. Rates, pathways and drivers for peatland development in the Hudson Bay Lowlands, northern Ontario, Canada. Journal of Ecology 92, 1036-1053.

Grant, K.M., Rohling, E.J., Ramsey, C.B., Cheng, H., Edwards, R.L., Florindo, F., Heslop, D., Marra, F., Roberts, A.P., Tamisiea, M.E., Williams, F., 2014. Sea-level variability over five glacial cycles. Nature communications 5, 5076.

Grunsky, E.C., 2010. The interpretation of geochemical survey data. Geochemistry: Exploration, Environment, Analysis 10, 27-74.

Heiri, O., Lotter, A.F., Lemcke, G., 2001. Loss on ignition as a method for estimating organic and carbonate content in sediments: reproducibility and comparability of results. Journal of Paleolimnology 25, 101-110.

Helmens, K., Engels, S., 2010. Ice-free conditions in eastern Fennoscandia during early Marine Isotope Stage 3: lacustrine records. Boreas 39, 399-409.

Helmens, K.F., 2014. The Last Interglacial–Glacial cycle (MIS 5–2) re-examined based on long proxy records from central and northern Europe. Quaternary Science Reviews 86, 115-143.

Juggins, S., 2015. rioja: Analysis of Quaternary Science Data. R package version (0.9-5), http://cran.r-project.org/package=rioja.

Kapp, R.O., Davis, O.K., King, J.E., 2000. Ronald O. Kapp's Pollen and Spores, 2nd edition ed, College Station, Texas, USA.

Kleinen, T., Brovkin, V., Munhoven, G., 2015. Carbon cycle dynamics during recent interglacials. Climate of the Past Discussions 11, 1945-1983.

778 Kleman, J., Jansson, K., De Angelis, H., Stroeven, A.P., Hättestrand, C., Alm, G., Glasser, N.,
779 2010. North American Ice Sheet build-up during the last glacial cycle, 115–21kyr.
780 Quaternary Science Reviews 29, 2036-2051.
781 Lee, H.A., 1960. Late Glacial and Postglacial Hudson Bay Sea Episode. Science 131, 1609-
782 1611.
783 MacDonald, B.G., 1969. Glacial and interglacial stratigraphy, Hudson Bay Lowlands,
784 Geological Survey of Canada Paper 65-23, pp. 78-99.
785 MacDonald, B.G., 1971. Late Quaternary stratigraphy and deglaciation in eastern Canada, The
786 late Cenozoic Glacial Ages. Yale Univeristy Press, pp. 331-353.
787 Mallinson, D., Burdette, K., Mahan, S., Brook, G., 2008. Optically stimulated luminescence age
788 controls on late Pleistocene and Holocene coastal lithosomes, North Carolina, USA.
789 Quaternary Research 69, 97-109.
790 McAndrews, J.H., Berti, A.A., Norris, G., 1973. Key to the Quaternary Pollen and Spores of the
791 Great Lakes Region. Royal Ontario Museum, Toronto, Canada.
792 McAndrews, J.H., Riley, J.L., Davis, A.M., 1982. Vegetation history of the Hudson Bay
793 Lowland: A postglacial pollen diagram from the Sutton Ridge. Naturaliste Canadien 109,
794 597-608.
795 McMartin, I., Dredge, L.A., Grunsky, E., Pehrsson, S., 2016. Till Geochemistry in West-Central
796 Manitoba: Interpretation of Provenance and Mineralization Based on Glacial History and
797 Multivariate Data Analysis. Economic Geology 111, 1001-1020.
798 Mott, R.J., DiLabio, R.N.W., 1990. Paleoecology of Organic Deposits of Probable Last
799 Interglacial Age in Northern Ontario. Géographie physique et Quaternaire 44, 309.

800 Murray, A.S., Wintle, A.G., 2003. The single aliquot regenerative dose protocol: potential for
801 improvements in reliability. Radiation Measurements 37, 377-381.
802 Natural Resources Canada, 2015. Obtain climate estimates at your locations. Government of
803 Canada. http://gmaps.nrcan.gc.ca/cl_p/climatepoints.php.
804 Nielsen, E., Morgan, A.V., Morgan, A., Mott, R.J., Rutter, N.W., Causse, C., 1986. Stratigraphy,
805 paleoeology, and glacial history of the Gillam area, Manitoba. Canadian Journal of Earth
806 Sciences 23, 1641-1661.
807 O'Reilly, B.C., Finkelstein, S.A., Bunbury, J., 2014. Pollen-Derived Paleovegetation
808 Reconstruction and Long-Term Carbon Accumulation at a Fen Site in the Attawapiskat
809 River Watershed, Hudson Bay Lowlands, Canada. Arctic, Antarctic, and Alpine Research
810 46, 6-18.
811 Oksanen, J., Blanchet, F.G., Kindt, R., Legendre, P., Minchin, P.R., O'Hara, R.B., Simpson,
812 G.L., Solymos, P., Stevens, M.H.H., Wagner, H., 2015. vegan: Community Ecology
813 Package. R package version 2.2-1, http://CRAN.R-project.org/package=vegan.
814 Ontario Geological Survey, 2015. Geology and selected mineral deposits of Ontario. Queen's
815 Printer for Ontario, Ontario, Canada.
816 Ontario Water Resources Commission, 1969. Data for Northern Ontario water resource studies
817 1966 to 1968 Water Resources Bulletin 1-1, Toronto, Ontario.
818 Overpeck, J.T., Webb, T., III, Prentice, I.C., 1985. Quantitative Interpretation of Fossil Pollen
819 Spectra: Dissimilarity Coefficients and the Method of Modern Analogs. Quaternary
820 Research 23, 87-108.

821 Parent, M., Paradis, S.J., Bolsvert, E., 1995. Ice-flow patterns and glacial transport in the eastern
822 Hudson Bay region: implications for the late Quaternary dynamics of the Laurentide Ice
823 Sheet. Canadian Journal of Earth Sciences 32, 2057-2070.
824 Pico, T., Creveling, J.R., Mitrovica, J.X., 2017. Sea-Level Records from the U.S. Mid-Atlantic
825 Constrain Laurentide Ice Sheet Extent During Marine Isotope Stage 3. Nature
826 communications 8, 15612 / DOI 15610.11038/ncomms15612.
827 Pico, T., Mitrovica, J.X., Ferrier, K.L., Braun, J., 2016. Global ice volume during MIS 3 inferred
828 from a sea-level analysis of sedimentary core records in the Yellow River Delta.
829 Quaternary Science Reviews 152, 72-79.
830 Prescott, J.R., Hutton, J.T., 1994. Cosmic ray contributions to dose rates for luminescence and
831 ESR dating: Large depths and long-term time variations. Radiation Measurements 23,
832 497-500.
833 R Core Team, 2014. R: A language and environment for statistical computing. R Foundation for
834 Statistical Computing, Vienna, Austria.
835 Reimer, P.J., Bard, E., Bayliss, A., Beck, J.W., Blackwell, P.G., Bronk Ramsey, C., Buck, C.E.,
836 Cheng, H., Edwards, R.L., Friedrich, M., Grootes, P.M., Guilderson, T.P., Haflidason, H.,
837 Hajdas, I., Hatté, C., Heaton, T.J., Hoffmann, D.L., Hogg, A.G., Hughen, K.A., Kaiser,
838 K.F., Kromer, B., Manning, S.W., Niu, M., Reimer, R.W., Richards, D.A., Scott, E.M.,
839 Southon, J.R., Staff, R.A., Turney, R.S.M., van der Plicht, J., 2013. IntCal13 and
840 Marine13 Radiocarbon Age Calibration Curves 0–50,000 Years cal BP. Radiocarbon 55,
841 1869-1887.
842 Rémillard, A.M., Hétu, B., Bernatchez, P., Bertran, P., Fisher, T.G., 2013. The Drift des
843 Demoiselles on the Magdalen Islands (Québec, Canada): sedimentological and

micromorphological evidence of a Late Wisconsinan glacial diamict. Canadian Journal of Earth Sciences 50, 545-563.

Rémillard, A.M., St-Onge, G., Bernatchez, P., Hétu, B., Buylaert, J.-P., Murray, A.S., Vigneault, B., 2016. Chronology and stratigraphy of the Magdalen Islands archipelago from the last glaciation to the early Holocene: new insights into the glacial and sea-level history of eastern Canada. Boreas 45, 604-628.

Richerol, T., Fréchette, B., Rochon, A., Pienitz, R., 2016. Holocene climate history of the Nunatsiavut (northern Labrador, Canada) established from pollen and dinoflagellate cyst assemblages covering the past 7000 years. The Holocene 26, 44-60.

Riley, J.L., 2011. Wetlands of the Hudson Bay Lowland: an Ontario overview Nature Conservancy of Canada, Toronto, ON.

Sanford, R.F., Pierson, C.T., Crovelli, R.A., 1993. An objective replacement method for censored geochemical data. Mathematical Geology 25, 59-80.

Schaetzl, R.J., Forman, S.L., 2008. OSL ages on glaciofluvial sediment in northern Lower Michigan constrain expansion of the Laurentide ice sheet. Quaternary Research 70, 81-90.

Simpson, G.L., 2007. Analogue Methods in Palaeoecology: Using the analogue Package. Journal of Statistical Software 22, 1-29.

Simpson, G.L., Oksanen, J., 2014. analogue: Analogue matching and Modern Analogue Technique transfer function models. R package version 0.14-0, http://cran.r-project.org/package=analogue.

Sionneau, T., Bout-Roumazeilles, V., Meunier, G., Kissel, C., Flower, B.P., Bory, A., Tribovillard, N., 2013. Atmospheric re-organization during Marine Isotope Stage 3 over

the North American continent: sedimentological and mineralogical evidence from the Gulf of Mexico. Quaternary Science Reviews 81, 62-73.

Skinner, R.G., 1973. Quaternary stratigraphy of the Moose River Basin, Ontario. Geological Survey of Canada Bulletin 225, 1-77.

Stuiver, M., Heusser, C.J., Yang, I.C., 1978. North American Glacial History Extended to 75,000 Years Ago. Science 200, 16-21.

Stuiver, M., Reimer, P.J., 1993. Extended ^{14}C data base and revised Calib 3.0 ^{14}C age calibration program. Radiocarbon 35, 215-230.

Terasmae, J., Hughes, O.L., 1960. A palynological and geological study of Pleistocene deposits in the James Bay Lowlands, Ontario (45 N1/2). Geological Survey of Canada Bulletin 62, 1-15.

Thorleifson, L.H., Wyatt, P.H., Shilts, W.W., 1992. Hudson Bay lowlands Quaternary stratigraphy: Evidence for early Wisconsinan glaciation centred in Quebec, Special Paper 270. Geological Society of America, pp. 207-221.

Thorleifson, L.H., Wyatt, P.H., Warman, T.A., 1993. Quaternary stratigraphy of the Severn and Winisk drainage basins, Northern Ontario. Geological Survey of Canada.

Ullman, D.J., LeGrande, A.N., Carlson, A.E., Anslow, F.S., Licciardi, J.M., 2014. Assessing the impact of Laurentide Ice Sheet topography on glacial climate. Climate of the Past 10, 487-507.

Väliranta, M., Birks, H.H., Helmens, K., Engels, S., Piirainen, M., 2009. Early Weichselian interstadial (MIS 5c) summer temperatures were higher than today in northern Fennoscandia. Quaternary Science Reviews 28, 777-782.

889 Väliranta, M., Salonen, J.S., Heikkila, M., Amon, L., Helmens, K., Klimaschewski, A., Kuhry,
890 P., Kultti, S., Poska, A., Shala, S., Veski, S., Birks, H.H., 2015. Plant macrofossil
891 evidence for an early onset of the Holocene summer thermal maximum in northernmost
892 Europe. Nature communications 6, 6809.
893 Veillette, J.J., Dyke, A.S., Roy, M., 1999. Ice-flow evolution of the Labrador Sector of the
894 Laurentide Ice Sheet: a review, with new evidence from northern Quebec. Quaternary
895 Science Reviews 18, 993-1019.
896 Veillette, J.J., Pomares, J.-S., 1991. Older ice flows in the Matagami-Chapais area Quebec.
897 Geological Survey of Canada, Paper 91-1C Current Research, part C, 143-148.
898 Wainer, K.A.I., Rowe, M.P., Thomas, A.L., Mason, A.J., Williams, B., Tamisiea, M.E.,
899 Williams, F.H., Düsterhus, A., Henderson, G.M., 2017. Speleothem evidence for MIS 5c
900 and 5a sea level above modern level at Bermuda. Earth and Planetary Science Letters
901 457, 325-334.
902 Whitmore, J., Gajewski, K., Sawada, M., Williams, J.W., Shuman, B., Bartlein, P.J., Minckley,
903 T., Viau, A.E., Webb, T., III, , Anderson, P.M., Brubaker, L.B., 2005. North American
904 and Greenland modern pollen data for multi-scale paleoecological and paleoclimatic
905 applications. Quaternary Science Reviews 24, 1828-1848.
906 Wintle, A.G., Murray, A.S., 2006. A review of quartz optically stimulated luminescence
907 characteristics and their relevance in single-aliquot regeneration dating protocols.
908 Radiation Measurements 41, 369-391.
909 Wood, J.R., Forman, S.L., Everton, D., Pierson, J., Gomez, J., 2010. Lacustrine sediments in
910 Porter Cave, Central Indiana, USA and possible relation to Laurentide ice sheet marginal

911 positions in the middle and late Wisconsinan. Palaeogeography, Palaeoclimatology,
912 Palaeoecology 298, 421-431.
913 Zabenskie, S., 2006. Postglacial Climatic Change on Boothia Peninsula, Nunavut, Canada, M.Sc.
914 thesis, Department of Geography. University of Ottawa.

915